



## EFFECT OF MORPHOLOGY ON THE ARSENIC REMOVAL OF IRON OXIDE

Nguyen Nhat Huy<sup>1</sup>, Le Tri Thich<sup>2</sup>, Phan Phuoc Toan<sup>1,2</sup>, Nguyen Trung Thanh<sup>2</sup>

<sup>1</sup>Ho Chi Minh City University of Technology, VNU-HCM

<sup>2</sup>An Giang University, VNU-HCM

### Information:

Received: 24/01/2020

Accepted: 18/06/2020

Published: 04/2021

### Keywords:

Iron oxide, arsenic removal, adsorbent, water treatment

### ABSTRACT

*In this study, iron oxide nanomaterials with urchin-like and cubic shapes were synthesized by microwave-assisted hydrothermal method with and without ethylene glycol surfactant. The produced materials were then characterized by X-ray diffraction, transmission electron microscopy, and Fourier-transform infrared spectroscopy. The arsenic adsorption efficiency and capacity were employed as indicators for evaluating the applicability of the products and the effect of their morphology. Results showed that appropriate adsorption conditions for urchin-like and cubic iron oxides were pH 6 - 7 and pH 8, respectively, with high adsorption capacities of 11.7 and 11.1 mg/g, indicating that these materials are very potential for arsenic removal in groundwater and wastewater.*

## 1. INTRODUCTION

Arsenic pollution of groundwater is a serious problem of drinking water supply in many areas of Vietnam (Berg *et al.*, 2001), especially in the Mekong delta region (Buschmann *et al.*, 2008). Since arsenic compounds cannot be decomposed, the removal of arsenic mainly focuses on the oxidation of As(III) to As(V) followed by phase separation of As(V) precipitate. Practically, As(III) can be oxidized by natural air or strong oxidants such as ozone, potassium permanganate, or hydrogen peroxide to form As(V). After that, phase separation can be done by traditional chemical water treatment (e.g. coagulation, precipitation, sand filtration, and ion exchange), electrocoagulation, membrane technology (e.g., nanofiltration, reverse osmosis, and electrodialysis), and

adsorption by nanomaterials (Nidheesh and Singh, 2017; Bissen and Frimmel, 2003; Kowalski, 2014; Shih, 2005; Jiang, 2001; Vu *et al.*, 2003; Ning, 2002). Among them, adsorption emerges as one of the most effective methods for the removal of arsenic in drinking water (Chiban *et al.*, 2012; Baig *et al.*, 2015; Mohan and Pittman Jr, 2007; Lata and Samadder, 2016). Recently, iron oxide nanomaterial has attracted considerable attention for arsenic removal due to its various morphologies, large surface area, high amount of active sites, and magnetic property (Gallegos-Garcia *et al.*, 2012; Siddiqui and Chaudhry, 2017; Luong *et al.*, 2018). However, there has been very limited information on the effect of morphology on the adsorption capacity of iron oxide for arsenic removal.

In this work, we aimed to synthesize two types of iron oxide and applied them for arsenic removal in groundwater. The objectives of this study include to (1) determine the morphological characteristics of iron oxide nanomaterials synthesized in the presence and absence of ethylene glycol surfactant; (2) evaluate the effect of morphology of iron oxide nanomaterials on arsenic adsorption efficiency in actual groundwater sample through two experimental factors: contact time and initial solution pH.

## 2. MATERIALS AND METHODS

Chemicals such as HNO<sub>3</sub>, HCl, urea, ethylene glycol, and NaOH were from China. The stock arsenic solution, KBr, and iron precursor (i.e. FeCl<sub>3</sub> and Fe(NO<sub>3</sub>)<sub>3</sub>) were from Merck (Germany). The water used in this study was double distilled water. Samples of arsenic contaminated groundwater were actually taken from An Phu district, An Giang province. The sample was pretreated by aerating with air for 15 minutes to oxidize iron and transform As (III) to As (V). The average arsenic concentration was determined to be 50 ppb and used directly in adsorption experiments.

Iron oxide nanomaterials were synthesized by microwave-assisted hydrothermal method with and without using surfactant of ethylene glycol (EG). In a typical procedure, 6 mmol of urea and 6 mmol of FeCl<sub>3</sub>.H<sub>2</sub>O were dissolved in a beaker containing 45 mL of water and 15 mL of EG (or 60 mL of water without EG), followed by stirring until transparent color appeared and treating in a microwave for 30 min. The materials were then rinsed and centrifuged twice, and finally dried at 80 °C for 4 h and named as EG-Fe<sub>x</sub>O<sub>y</sub> (with EG) and W-Fe<sub>x</sub>O<sub>y</sub> (without EG). The materials were then characterized by Fourier-transform infrared spectroscopy (FTIR), X-ray diffraction (XRD), and transmission electron microscopy (TEM).

Arsenic removal was conducted using batch adsorption tests. The effects of environmental factors on the arsenic removal were investigated, including pH (4 – 8) and adsorption time (15 – 75 min). Arsenic concentration in the supernatant was measured by an atomic absorption spectrophotometer (ZEEnit 700, Analytik Tena, Germany) or ICP-AES. The arsenic adsorption capacity of iron oxide is calculated by Equation 1.

$$q = \frac{(C_i - C_e) \times V}{m} \quad (1)$$

Where  $q$  (mg/g) is the adsorption capacity;  $C_i$  and  $C_e$  (mg/L) the initial and equilibrium concentrations of arsenic;  $V$  (L) adsorption volume; and  $m$  (g) amount of adsorbent.

## 3. RESULTS AND DISCUSSION

Figure 1 presents the FTIR spectra of iron oxide synthesized with and without EG. It can be observed that the FTIR spectra of both materials were similar and characteristic for Fe-O vibration of iron oxide with a band from 575 to 707 cm<sup>-1</sup> (Zhou *et al.*, 2012) and 1650 cm<sup>-1</sup> (Aswin Kumar and Viswanathan, 2018). The bands from 3434 to 3424 cm<sup>-1</sup> are OH groups on the surface of the material (Aswin Kumar and Viswanathan, 2018). These clear and sharp peaks indicate the abundance of surface OH group, which is favorable for adsorption and ion exchange.

As seen in Figure 2, both materials have a crystalline phase of Fe<sub>2</sub>O<sub>3</sub> (Du *et al.*, 2009). Besides that, the peaks at  $2\theta$  of 35.28, 36.18, 43.3, and 54.48° on both materials are assigned for  $\alpha$ -Fe<sub>2</sub>O<sub>3</sub> and  $\gamma$ -Fe<sub>2</sub>O<sub>3</sub> phases simultaneously (Ning *et al.*, 2017), where the highest intensity peak at  $2\theta$  of 36.18° is attributed to (311) plane (Wu *et al.*, 2015). The crystalline sizes calculated from XRD results using the Scherrer equation were 36.18 and 32.4 nm for iron oxides synthesized with and without EG, respectively. Moreover, both FTIR and XRD

results confirmed the high purity of iron oxide in these two materials without impurity peaks.

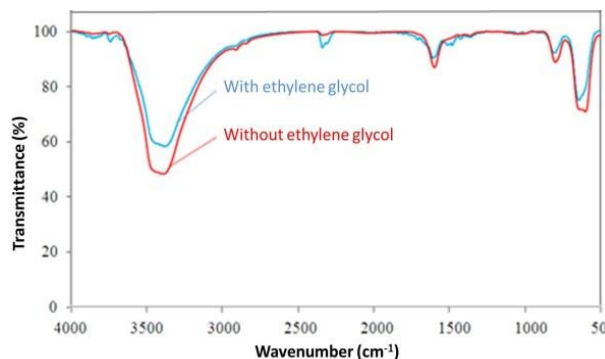


**Figure 1. FTIR spectra of iron oxide synthesized with and without EG**

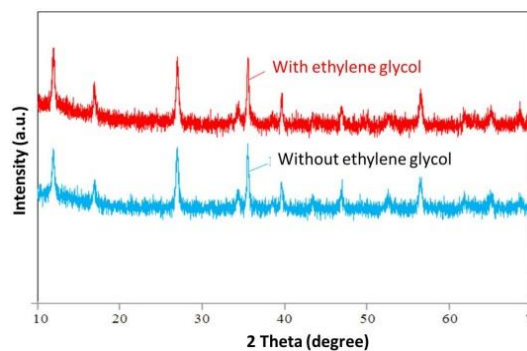


**Figure 2. XRD pattern of iron oxide synthesized with and without EG**

TEM images of iron oxides synthesized with and without EG are displayed in Figure 3. With highly dispersed particles, the TEM revealed the remarkable difference between the two materials. While W-Fe<sub>x</sub>O<sub>y</sub> had a cubic shape with a size of 10 nm, EG-Fe<sub>x</sub>O<sub>y</sub> showed urchin-

like shape, symmetric nanostructure, and relative uniform particle size of 30 nm, which is consistent with XRD results. This could be explained by the micelle structure created by water – ethylene glycol mixture during the synthesis of EG-Fe<sub>x</sub>O<sub>y</sub>.

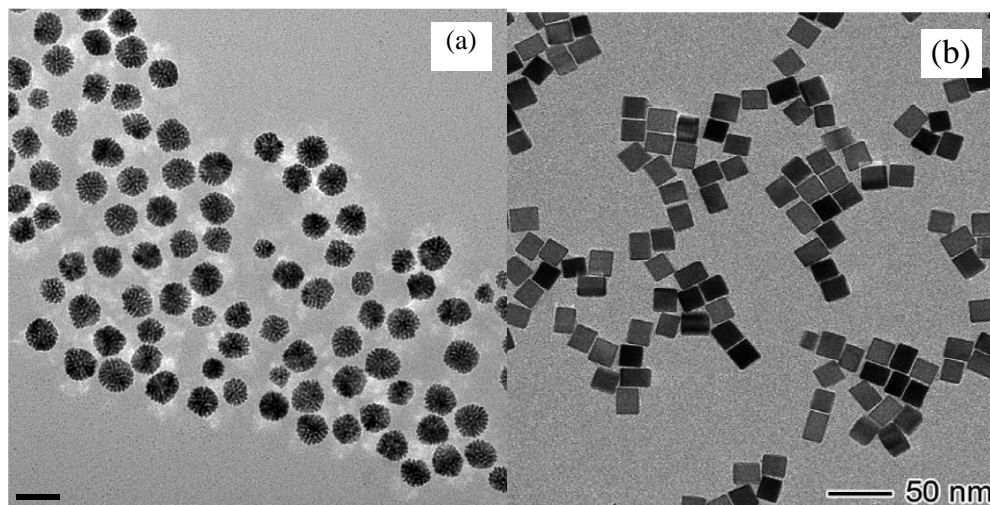


**Figure 3. TEM images of (a) EG-Fe<sub>x</sub>O<sub>y</sub> and (b) W-Fe<sub>x</sub>O<sub>y</sub>**

The effects of pH and adsorption time on the adsorption capacity of iron oxides for arsenic removal are illustrated in Figure 4. For EG-Fe<sub>x</sub>O<sub>y</sub>, the appropriate pH range for adsorption was found to be 6 – 7 with an efficiency of over 86%, as in Figure 4(a). Lower or higher pH values decreased the adsorption efficiency since the surface of iron oxide is protonated at highly acidic conditions while formed hydrated

complex at the highly basic condition. For W-Fe<sub>x</sub>O<sub>y</sub>, the appropriate pH was found at pH 8 due to its flat surface, which could produce more surface OH group at higher pH value. Figure 4(b) demonstrates the effect of adsorption time on arsenic removal, indicating that 15 min is sufficient equilibrium time for the adsorption with high arsenic removal efficiency of 88%. The arsenic adsorption

capacity of EG-Fe<sub>x</sub>O<sub>y</sub> and W-Fe<sub>x</sub>O<sub>y</sub> were calculated to be 11.7 mg/g at pH 6-7 and 11.1 mg/g at pH 8, respectively. Therefore, EG-

Fe<sub>x</sub>O<sub>y</sub> is suitable for arsenic removal in groundwater at low pH while W-Fe<sub>x</sub>O<sub>y</sub> for wastewater at high pH value.

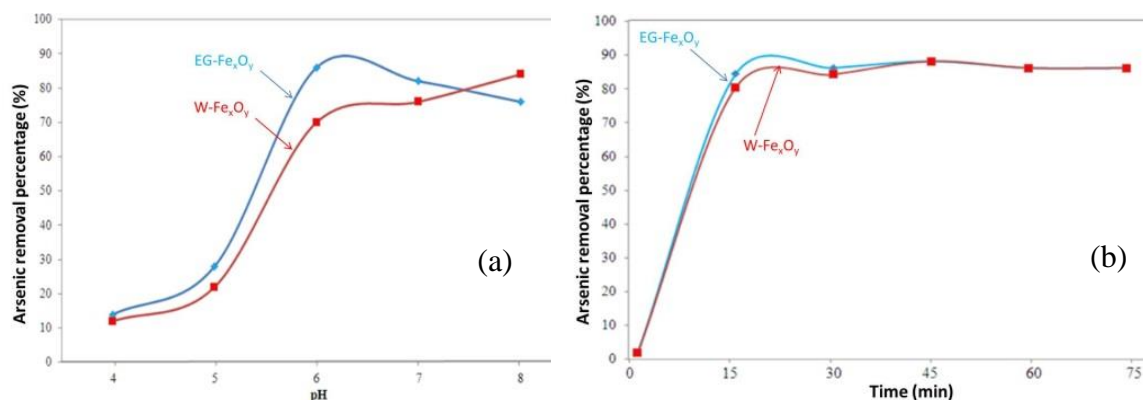


Figure 4. Effect of (a) pH and (b) adsorption time on arsenic adsorption efficiency

The used EG-Fe<sub>x</sub>O<sub>y</sub> adsorbent was collected, dried at 105 °C, and characterized by FTIR in order to find the structural change and propose the adsorption mechanism. The FTIR spectra of fresh and used materials are plotted in Figure 5. There was a significant change in the surface of adsorbent with the decrease of OH group at wavenumber of 3434 and 712 cm<sup>-1</sup> and the

appearance of peaks at 865 cm<sup>-1</sup> of As-O (Goldberg and Johnston, 2001) and 1384 cm<sup>-1</sup> of O-N vibrations (Smidt *et al.*, 2011; Song *et al.*, 2012), proving the adsorption of arsenic and nitrate from groundwater. These also implies that the chemical adsorption of arsenic by surface OH group is the main mechanism for arsenic removal.

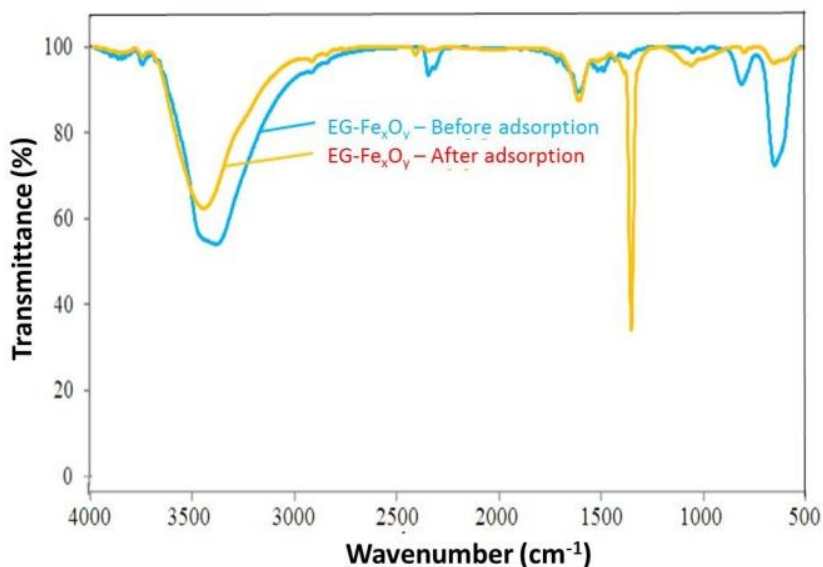


Figure 5. FTIR of fresh and used iron oxide

#### 4. CONCLUSIONS

Iron oxide nanomaterials were successfully synthesized by microwave-assisted hydrothermal method. The morphology of the

product strongly depended on the use of ethylene glycol surfactants. Urchin-like shape with a size of 30 nm and cubic shape with a size of 10 nm were obtained in the presence and absence of the surfactant, respectively. In the arsenic removal test, the adsorption capacities of urchin-like and cubic iron oxides were 11.7 mg/g at pH 6 – 7 and 11.1 mg/g at pH 8, respectively, after 15 min of adsorption. The adsorption mechanism was found to be the exchange of hydroxide groups on the surface of iron oxide with As cations.

#### ACKNOWLEDGMENTS

Many thanks are given to An Giang University and Vietnam National University - Ho Chi Minh City due to their support came from apparatus.

#### REFERENCES

- Aswin Kumar, I. & Viswanathan, N. (2018). Development and reuse of amine-grafted chitosan hybrid beads in the retention of nitrate and phosphate. *Journal of Chemical Engineering Data*, 63(1), 147-158.
- Baig, S. A., Sheng, T., Hu, Y., Xu, J. & Xu, X. (2015). Arsenic removal from natural water using low cost granulated adsorbents: a review. *CLEAN–Soil, Air, Water*, 43(1), 13-26.
- Berg, M., Tran, H. C., Nguyen, T. C., Pham, H. V., Schertenleib, R. & Giger, W. (2001). Arsenic contamination of groundwater and drinking water in Vietnam: a human health threat. *Environ. Sci. Technol.*, 35(13), 2621-2626.
- Bissen, M. & Frimmel, F. H. (2003). Arsenic— a review. Part II: oxidation of arsenic and its removal in water treatment. *Acta Hydroch. Hydrob.*, 31(2), 97-107.
- Buschmann, J., Berg, M., Stengel, C., Winkel, L., Sampson, M. L., Trang, P. T. K. & Viet, P. H. (2008). Contamination of drinking water resources in the Mekong delta floodplains: Arsenic and other trace metals pose serious health risks to population. *Environ. Int.*, 34(6), 756-764.
- Chiban, M., Zerbet, M., Carja, G. & Sinan, F. (2012). Application of low-cost adsorbents for arsenic removal: A review. *Journal of Environmental Chemistry and Ecotoxicology*, 4(5), 91-102.
- Du, W., Sun, Q., Lv, X. & Xu, Y. (2009). Enhanced activity of iron oxide dispersed on bentonite for the catalytic degradation of organic dye under visible light. *Catal Commun*, 10(14), 1854-1858.
- Gallegos-Garcia, M., Ramírez-Muñiz, K. & Song, S. (2012). Arsenic removal from water by adsorption using iron oxide minerals as adsorbents: a review. *Miner. Process. Extr. Metall. Rev.*, 33(5), 301-315.
- Goldberg, S. & Johnston, C. T. (2001). Mechanisms of arsenic adsorption on amorphous oxides evaluated using macroscopic measurements, vibrational spectroscopy, and surface complexation modeling. *J. Colloid Interface Sci.*, 234(1), 204-216.
- Jiang, J.-Q. (2001). Removing arsenic from groundwater for the developing world—a review. *Water Sci. Technol.*, 44(6), 89-98.
- Kowalski, K. P. Chapter 8 - Advanced Arsenic Removal Technologies Review. In: SØGAARD, E. G. (ed.) *Chemistry of Advanced Environmental Purification Processes of Water*. Amsterdam: Elsevier; 2014. p. 285-337.
- Lata, S. & Samadder, S. R. (2016). Removal of arsenic from water using nano adsorbents and challenges: A review. *J. Environ. Manage.*, 166, 387-406.
- Luong, V. T., Cañas Kurz, E. E., Hellriegel, U., Luu, T. L., Hoinkis, J. & Bundschuh, J.

- (2018). Iron-based subsurface arsenic removal technologies by aeration: A review of the current state and future prospects. *Water Res.*, 133, 110-122.
- Mohan, D. & Pittman Jr, C. U. (2007). Arsenic removal from water/wastewater using adsorbents—a critical review. *J. Hazard. Mater.*, 142(1-2), 1-53.
- Nidheesh, P. V. & Singh, T. S. A. (2017). Arsenic removal by electrocoagulation process: Recent trends and removal mechanism. *Chemosphere*, 181, 418-432.
- Ning, R. Y. (2002). Arsenic removal by reverse osmosis. *Desalination*, 143(3), 237-241.
- Ning, W., Wang, T., Chen, H., Yang, X. & Jin, Y. (2017). The effect of Fe<sub>2</sub>O<sub>3</sub> crystal phases on CO<sub>2</sub> hydrogenation. *PloS one*, 12(8), e0182955.
- Shih, M.-C. (2005). An overview of arsenic removal by pressure-driven membrane processes. *Desalination*, 172(1), 85-97.
- Siddiqui, S. I. & Chaudhry, S. A. (2017). Iron oxide and its modified forms as an adsorbent for arsenic removal: A comprehensive recent advancement. *Process Saf. Environ. Prot.*, 111, 592-626.
- Smidt, E., Böhm, K. & Schwanninger, M. The application of FT-IR spectroscopy in waste management. Fourier transforms-new analytical approaches and FTIR strategies. InTech; 2011. p.
- Song, H., Zhou, Y., Li, A. & Mueller, S. (2012). Selective removal of nitrate from water by a macroporous strong basic anion exchange resin. *Desalination*, 296, 53-60.
- Vu, K. B., Kaminski, M. D. & Nuñez, L. 2003. Review of arsenic removal technologies for contaminated groundwaters. Argonne National Lab., IL (US).
- Wu, H., Wu, G. & Wang, L. (2015). Peculiar porous  $\alpha$ -Fe<sub>2</sub>O<sub>3</sub>,  $\gamma$ -Fe<sub>2</sub>O<sub>3</sub> and Fe<sub>3</sub>O<sub>4</sub> nanospheres: facile synthesis and electromagnetic properties. *Powder Technol.*, 269, 443-451.
- Zhou, Q., Wang, X., Liu, J. & Zhang, L. (2012). Phosphorus removal from wastewater using nano-particulates of hydrated ferric oxide doped activated carbon fiber prepared by Sol–Gel method. *Chem. Eng. J.*, 200-202, 619-626.